Valproic acid mediates miR-124 to down-regulate a novel protein target, GNAI1

Hirotaka Oikawa [a], Wilson W.B. Goh [b, c], Vania K.J. Lim [a], Limsoon Wong [c], Judy C.G. Sng [a, d, *]

[a] Neuroepigenetics Laboratory, Singapore Institute for Clinical Sciences, Agency for Science and Technology (A*STAR), Singapore
[b] School of Pharmaceutical Science and Technology, Tianjin University, China
[c] School of Computing, National University of Singapore, Singapore
[d] Department of Pharmacology, Yong Loo Lin School of Medicine, National University of Singapore, Singapore

ARTICLE INFO

ABSTRACT

Valproic acid (VPA) is an anti-convulsant drug that is recently shown to have neuroregenerative therapeutic actions. In this study, we investigate the underlying molecular mechanism of VPA and its effects on *Bdnf* transcription through microRNAs (miRNAs) and their corresponding target proteins. Using *in silico* algorithms, we predicted from our miRNA microarray and iTRAQ data that miR-124 is likely to target at guanine nucleotide binding protein alpha inhibitor 1 (GNAI1), an adenylate cyclase inhibitor. With the reduction of GNAI1 mediated by VPA, the cAMP is enhanced to increase *Bdnf* expression. The levels of GNAI1 protein and *Bdnf* mRNA can be manipulated with either miR-124 mimic or inhibitor. In summary, we have identified a novel molecular mechanism of VPA that induces miR-124 to repress GNAI1. The implication of miR-124→GNAI1→BDNF pathway with valproic acid treatment suggests that we could repurpose an old drug, valproic acid, as a clinical application to elevate neurotrophin levels in treating neurodegenerative diseases.

1. Introduction

Traditionally, valproic acid (VPA) has been a first line of drug in treating epilepsy and manic disorder (Henry, 2003). Over the last decade, researchers have reported that VPA has other therapeutic actions beside its gamma-aminobutyric acid (GABA) enhancing effects (Rosenberg, 2007). VPA has also been shown to have efficacy in anti-tumorogenesis, neuroprotection, promoting neurogenesis, differentiation and neuroregeneration (Abematsu et al., 2010; Foti et al., 2013; Fukuchi et al., 2009; Hao et al., 2004; Jessberger et al., 2007; Laeng et al., 2004; Liu et al., 2012; Morris and Monteggia, 2013; Phiel et al., 2001). It has been reported to induce epigenetic changes such as inhibiting histone deacetylases (Jessberger et al., 2007; Tremolizzo et al., 2005) and microRNAs (Goh et al., 2011; Hunsberger et al., 2012; Zhou et al., 2008) that modulate gene expression changes post-transcriptionally. Such

epigenetic changes regulate genes that improve synaptic plasticity (Bredy et al., 2007; Calabrese et al., 2012; Silingardi et al., 2010).

MicroRNAs (miRNAs) are single-stranded noncoding RNAs (ncRNAs). They are approximately 22 nucleotides long and are cleaved by a nuclease, known as Dicer (Filipowicz et al., 2008; Novina and Sharp, 2004). miRNA attaches to an RNA interference-silencing complex (RISC) and is directed to the messenger RNA (mRNA) of interest. Because of the slight imperfections in the match between the miRNA and its recognition site, the miRNA forms a bulge, blocking the mRNA from being translated into protein (Chuang and Jones, 2007; Gangaraju and Lin, 2009). Together with ncRNAs, they interact with the epigenome to fine-tune the gene activity and regulate neuro-development and -physiological network integration (Cao et al., 2007; Nelson et al., 2008). Many miRNAs are expressed in the CNS and have been shown to regulate neuronal development, differentiation, synaptogenesis and plasticity (Edbauer et al., 2010; Fiore et al., 2011; Impey et al., 2010; Karr et al., 2009; Makeyev et al., 2007; Vo et al., 2005; Wayman et al., 2008; Yu et al., 2008). We have previously reported, from an *in silico* angle, under the influence of VPA, miRNAs interacts specifically with components of the protein–protein interaction networks that affect dendritic growth and synaptic plasticity (Goh

* Corresponding author. Neuroepigenetics Laboratory, Department of Pharmacology, Yong Loo Ling School of Medicine, MD3, 16 Medical Drive 04-01 (S) 117600, Singapore.
E-mail address: phcsngj@nus.edu.sg (J.C.G. Sng).

et al., 2011). We observed in VPA treatment increased dendritic branching and cortical rewiring (Lim et al., manuscript in submission) and thus hypothesized that disruption of such protein–protein networks could either be due to an increase in neurogenesis or neuronal differentiation.

In this study, we follow up by validating global changes in miRNAs and proteins after VPA administration taken from visual cortices. Among the candidate miRNAs identified, miR-124 is predicted to target guanine nucleotide binding protein alpha inhibitor 1 (GNAI1). GNAI1 is an adenylate cyclase inhibitor that modulates cAMP. Using a primary neuronal cortical culture as an *in vitro* model, we found that VPA induced miR-124 which in turn, repressed GNAI1. This consequently initiated cAMP leading to the increase in brain-derived neurotrophic factor (*Bdnf*). This gives us a better understanding of the mechanistic action of VPA. In addition, changes in the levels and activities of BDNF have been described in a number of neurodegenerative disorders. Using VPA could be an experimental strategy to enhance BDNF and our dissection of the molecular mechanism underlying VPA's effects may allow us to design more specific targeting strategies to aid in neuroregeneration.

2. Methods

2.1. Animals, animal welfare and ethical statement

Adult male C57BL/6 mice (postnatal age ~60 days) were used. Animals were maintained on a 12 h light/dark cycle and had access to food and water *ad libitum*. All animal protocols have been approved by the Institutional Animal Care and Use Committee (IACUC) in Biopolis Resource Centre, A*STAR (#120723) and National University of Singapore (#10–101).

2.2. Drug administration

Sodium valproate (Valproic acid) (VPA; 200 mgkg^{-1}, i.p.; Sigma–Aldrich) was dissolved in sterile saline. The same volume of vehicle solution was injected into control animals. VPA (VPA 2d) or vehicle solution (Veh 2d) was injected into C57BL/6 adult mice every 12 hourly over 2 days. Visual cortices were excised 12 h after the last injection.

2.3. Neuronal cultures

Primary neuronal cultures were prepared as described by di Porzio et al. (1980) with minor modifications. Briefly, embryonic mouse cerebral neocortices was dissected from fetal C57BL/6 mice at 17–18-days of gestation. The dissected tissues were incubated at room temperature with versene (GIBCO) for 12 min followed by mechanical dissociation. Dissociated cell suspensions were plated at a density of 2.0×10^5 cells/cm^2 on plastic tissue culture dish coated with poly-L-lysine and kept in a defined medium (Neurobasal/B-27; GIBCO) supplemented with glucose (33 mM), glutamine (2 mM), penicillin (100 U/ml) and streptomycin (100 μg/ml). Cultures were maintained in a humidified 5% CO$_2$ incubator at 37 °C for either 3 days *in vitro* (DIV) or 6 DIV with addition of 10 mM cytosine arabinoside (Sigma Aldrich) on 2 DIV to inhibit glial proliferation. Under these conditions, cultures contained ~95% neurons.

2.4. Reagents and antibodies

in sterile saline and either vehicle or VPA was injected intraperitoneally at 200 mgkg^{-1} (derived from human equivalent dose human mg/kg dose = (mouse mg/kg dose × mouse K$_m$)/

human K$_m$) into C57BL/6 mice either 2 h after the first drug administration (Veh 2h or VPA 2h) or every 12 hourly over 2 days (Veh 2d or VPA 2d). For the *in vitro* experiment, valproic acid was dissolved in saline and 3 DIV primary neuronal cultures were treated with either Veh or 5 mM VPA (concentration equivalent to *in vivo* concentration; WinNolin software; and (Fukuchi et al., 2009)) for 12 h prior to analysis. 100 nM of has-miR-124-3p inhibitor (Exiqon) and 100 nM of miR-124 mimic (QIAGEN) with their respective negative controls was applied to 3 DIV primary neuronal culture (density of 2.0×10^5 cells/cm^2) and incubated for another 3 DIV before using them for experiment. For western blots, primary antibodies-Guanine nucleotide-binding protein G(i), alpha-1 subunit, GNAI1 (SAB2100936; Sigma Aldrich): 1:1000 for Western Blotting (WB); beta III tubulin (β-tubulin; T0198; Sigma Aldrich): 1:1000 for WB. Secondary antibodies-Goat anti-Rabbit IRDye® 800CW (926–32211; Li-Cor Biosciences): 1:3000 for WB; Alexa Fluor® 680 goat anti-mouse IgG (A21076; Invitrogen): 1:3000 for WB. For cAMP assay, cAMP was measured with High Sensitivity Direct Cyclic AMP Chemiluminescent Immunoassay Kit (ArborAssays).

2.5. miRNA and mRNA preparation

Total RNA was isolated from visual cortices or primary neuronal cultures using miRCUR™ RNA isolation kit (Exiqon). For microarray experiment, independent pairs of visual cortices from 4 mice of each treatment were used as biological replicates. For every miRNA real-time quantitative PCR and mRNA real-time quantitative PCR, independent pairs of visual cortices and primary neuronal cultures were used as biological replicates and different set of samples from those used in the microarray were prepared for qPCR validation.

2.6. miRNA array profiling

The quality of the total RNA was first verified on an Agilent Bioanalyzer. Total RNA (700 ng) from sample and reference were labeled with Hy3™ and Hy5™ fluorescent label, respectively, using the miRCUR LNA™ Array power labelling kit (Exiqon) and hybridized to the miRCUR LNA™ array version 11.0 (Exiqon). After hybridization, the microarray slides were scanned using the Agilent G2565BA Microarray Scanner System (Agilent Technologies, Inc.) and the image analysis was carried out using the ImaGene 8.0 software (BioDiscovery, Inc.), background corrected with Normexp and normalized using the global Lowess (LOcally WEighted Scatterplot Smoothing) regression algorithm. Differentially expressed miRNAs were selected via t-test comparisons of control vs treatment (p-value ≤ 0.05). The expression scores were then pegged to a color gradient map on a scale from -2 (blue, low expression) to 2 (pink, high expression). Each individual square represents a pair of visual cortices from one biological replicate (n = 4 per treatment group).

2.7. miRNA and mRNA real time qPCR

Total RNA was converted to cDNA using miRCUR LNA™ Universal cDNA synthesis kit (Exiqon) and real-time qPCR was done using SYBR® Green primers for hsa-miR-22, hsa-miR-33a, hsa-miR-124, hsa-miR-132, U6 snRNA (hsa mmu), 5S rRNA (hsa), Bdnf I forward, 5′ -AGTTGCTTTGTCTTCTGTAGTCGC- 3′, and reverse, 5′ -CCTGGAG ACTCAGTGTCTTA- 3′ and *Gapdh* forward 5′ CTCCCAG-GAAGACCCTGCTT 3′, reverse 5′ GGAACAGGGAGGAGCAGAGA 3′) and SYBR® Green master mix (Exiqon). Real-time qPCR was also done using Taqman primers for *Gnai1* (Mm01165301_m1), *18S* (Hs99999901_s1), and *Gapdh* (Mm99999915_g1) and Taqman Mastermix. All RT-qPCR were done on the FAST7900HT machine

(Applied Biosystems) and analyzed with RQ manager (Applied Biosystems).

2.8. iTRAQ preparation and profiling

Isobaric tag for relative and absolute quantitation (iTRAQ) is a technique that allows a comprehensive comparative quantitative determination of protein expression (Ross et al., 2004) and we used the protocol as previously described (Goh et al., 2011). Nuclei-extracted proteins from Veh- and VPA-treated visual cortices (6—8 pooled samples, 200 μg each, 2 biological replicates) were separated via SDS-PAGE, excised, digested with trypsin and labeled with iTRAQ tags. The tagged peptides are then separated using Electrostatic Repulsion—Hydrophobic Interaction Chromatography (ERLIC) into 20 fractions. Each fraction was analyzed using a QStar Elite LC-MS/MS system (AB SciEx). Proteins and peptides were identified and quantified using ProteinPilot (Paragon) (v2.01) against the IPI mouse database. False discovery rates was deployed using target-decoy database search and set to ≤1%. The differential scores were obtained from the signals relative to the Vehicle after the multiplex of the Vehicle vs VPA samples and standardized cut off of >1.2 or <0.8 are used as previously described (Goh et al., 2011).

2.9. In silico miRNA target prediction

The candidate proteins were determined *in silico* from scores of TargetScan (Friedman et al., 2008), PicTar (Krek et al., 2005) and DIANA (Maragkakis et al., 2009). From the three computational algorithms, a combined precision f(t) was calculated from each precision score, P_i. From DIANA, a precision score indicates that the probability that the prediction is correct (the ratio of true positives (TP) over the sum of true positives and false positives (FP), or (TP/(TP + FP)). In DIANA, the average number of targets for mock miRNAs provided an estimate of the FP. In TargetScan the aggregate Pct score is the combined probability of all predicted target sites for a given miRNA to a target). Instead of a probability, PicTar provides a single score value. We convert this into a precision estimate by normalizing all prediction scores over the highest score.

For a target miRNA-target, assuming all precision scores in each database are independent, the combined precision score, f(t) is denoted by (Goh et al., 2011):

$$f(t) = 1 - (1 - P_{DIANA})(1 - P_{TargetScan})(1 - P_{PicTar})$$

2.10. Western Blotting

Dissected visual cortices and primary neuronal cultures were used. Whole cell lysates from these tissues were extracted and quantified (20 μg). Immunoblots were blocked with Odyssey blocking buffer (Li-Cor Biosciences) and probed with the appropriate dilutions of primary and secondary antibodies in Odyssey blocking buffer with supplementation by 0.05% Tween-20. The specificity of the antibodies was confirmed by western blot. The immunoreactive bands were visualized with Odyssey (Li-Cor Biosciences). Equal protein loading was verified by anti-β-tubulin antibody. The intensity of the western blot protein bands was carried out with Image J.

2.11. cAMP assay

The cAMP standard and reaction solutions were prepared according to manufacturer's protocol and added to the cell lysate. The

cAMP antibody was then added and left to incubate at room temperature for 2 h. The amount of chemiluminescence was measured on a chemiluminescent plate reader (Promega).

2.12. GenBank accession numbers

The miRNAs and proteomics discussed in this publication have been deposited in NCBI's Gene Expression Omnibus (GEO, http://www.ncbi.nlm.nih.gov/geo/) and are accessible through GEO series accession number (TBA).

2.13. Statistics

To evaluate qPCR and western blotting, we used GraphPad Prism 6. Significance evaluation is based on the paired-Student's *t*-test and corrected for multiple testing.

3. Results

3.1. Valproic acid differentially regulates microRNAs profile in mouse visual cortices

Valproic acid (VPA) has been shown to modulate epigenome landscape, such as HDAC inhibition, DNA methylation and miRNAs, thus changing gene expression to affect synaptic plasticity (Chuang and Jones, 2007; Goh et al., 2011; Putignano et al., 2007; Silingardi et al., 2010). We previously predicted through bioinformatics that miRNAs and protein—protein interaction network are dysregulated after VPA administration in the visual cortices (Goh et al., 2013; Goh et al., 2011). We first investigated the global changes in miRNAs in visual cortices after 2 h and 2 days of either vehicle (Veh 2h, Veh 2d) or valproic acid (VPA 2h, VPA 2d) administration using a commercial microarray analysis (Exiqon). The data is hierarchically clustered and cross-compared against the time points and treatments. VPA treatment produces a marked and distinctive expressional response that Veh samples are clearly segregated from the VPA samples (Suppl. Fig. 1). We next analyzed the differentially regulated miRNAs from the 2 day experiment (188 in total) using a two-sided *t*-test (p ≤ 0.05) and segregated them into significantly up- and down-regulated lists according to their p-value. Most of the miRNAs were up-regulated (136 out of 188; 72.3%, white sector, Fig. 1a) while 52 miRNAs were down-regulated (27.7%, black sector, Fig. 1a). We next selected four candidate up-regulated miRNAs, miR-22, miR-33a, miR-124 and miR-132 from the microarray, based on their ranking in the hierarchical clustering and their z-scores (Fig. 1b; miR-22: 11th; miR-124: 12th; miR-132: 53rd; miR-33a was interestingly not present with Veh and only up-regulated with VPA). Using a different set of Veh- or VPA-treated samples from those used in the microarray (n = 4 per treatment group), we confirmed their up-regulation *in vivo* by real-time-qPCR analysis. In agreement with the microarray data, miR-22 and miR-124 were significantly up-regulated (p = 0.0351 and p = 0.0229 respectively) and to a lesser extent, miR-33a and miR-132 (p = 0.0583 and p = 0.0592 respectively; Fig. 1c).

3.2. VPA also up-regulates candidate miRs-22, -33a, −124 and −132 in vitro

Parallel to our *in vivo* study, we stimulated 3 DIV mouse primary cortical neuronal culture with 5 mM VPA for 12 h and tested the selected miRNAs. This dose has been shown to epigenetically induce neuronal activity genes *in vitro* (Fukuchi et al., 2009). Indeed, all the candidate miRs-22, -33a, -124 and −132 were significantly up-regulated *in vitro*, agreeing with our *in vivo* data (Fig. 1d; miR-22, p = 0.0171; miR-22a, p = 0.0338; miR-124,
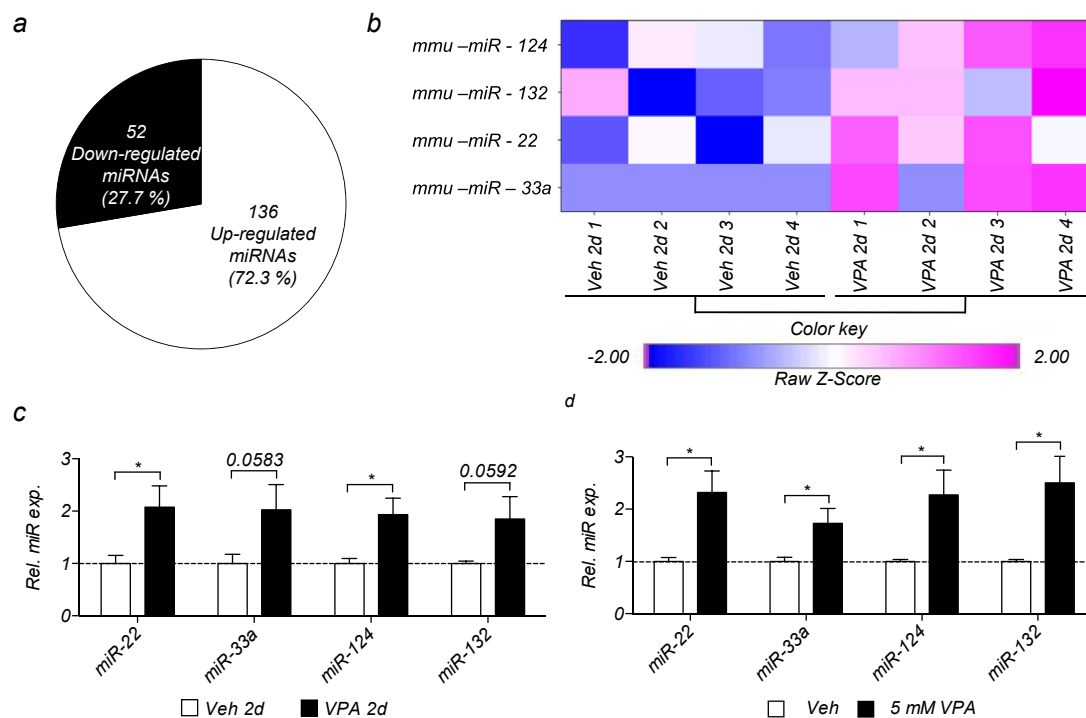
Fig. 1. Valproic acid differentially regulates microRNAs expression profile in both mouse visual cortices and primary neuronal cortical culture. (a) Pie chart showing differential expression of microRNAs (miRNAs) *in vivo* after 2 days of vehicle (Veh 2d) or valproic acid (VPA 2d) administration (up-regulated, white sector; down-regulated; black sector) obtained from microarray analysis. (b) Heat map representation of candidate miRNAs after Veh 2d or VPA 2d *in vivo* (blue, low expression; pink, high expression; each rectangle = biological replicate; n = 4 per treatment). (c) Validation of candidate miRNAs by real-time qPCR *in vivo* after Veh 2d or VPA 2d. (d) Validation of candidate miRNAs by real-time qPCR *in vitro* after Veh or VPA treatment (Veh, white bars, n = 3; VPA, black bars, n = 3). Data are represented as means ± s.e.m., normalized to *5S* and *U6* and relative to Veh, *p ≤ 0.05. (For interpretation of the references to colour in this figure legend, the reader is referred to the web version of this article.)

p = 0.0277; miR-132, p = 0.0248).

3.3. VPA differentially regulate global proteomic profile in mouse visual cortices

We compared the proteomic profile in mouse visual cortices between Veh 2d and VPA 2d. The *isobaric tags for relative and absolute quantitation* (*iTRAQ*) is a technique that allows a comprehensive comparative quantitative determination of protein expression from different sources in a single experiment. Nuclei-extracted proteins obtained from Veh- and VPA-treated dissected visual cortices (2 sets of 6—8 pooled samples in each treatment-total of 4 samples or lanes, with 200 μg protein per lane) were labeled into a 4-plex iTRAQ. The averaged differential scores from the two sets of pooled visual cortices proteins were calculated and segregated into either the up-regulated group with an average score over 1.25 or into the down-regulated group with an average score of less than 0.75. A total of 147 proteins met this criterion and 83 proteins were up-regulated (56.5%, white sector, Fig. 2a) while 64 proteins were down-regulated (43.5%, black sector, Fig. 2a).

3.4. miRNA-124 in silico prediction identifies GNAI1 as protein target

In order to have a better precision in predicting a regulatory microRNA to a target protein, we combined the predictions from three different *in silico* algorithms: TargetScan (http://www.targetscan.org/), PicTar (http://pictar.mdc-berlin.de/), and DIANA (http://diana.cslab.ece.ntua.gr) for all the four miRNAs against the down-regulated protein list obtained from iTRAQ. Among the four miRNAs, miR-124 gave the highest confidence score, based from its ranking on the microarray data and also its qPCR validation

in both *in vivo* and *in vitro* systems. miR-124 is the most abundant in the brain (Lagos-Quintana et al., 2002) and its expression is initiated upon different stages of neuro-genesis, -differentiation and -maturation in normal development (Lim et al., 2005; Makeyev et al., 2007), (Cao et al., 2007; Cheng et al., 2009; Papagiannakopoulos and Kosik, 2009; Sanuki et al., 2011; Visvanathan et al., 2007). Perturbation of miR-124 has been implicated in psychosis and neurodegenerative disorders (Das et al., 2013; Gong et al., 2013).

To date, target proteins of miR-124 are still not completely elucidated. Many of these are predicted based on a variety of techniques. However, most current miRNA-target prediction engines lack corroboration with each other, and the general accuracy is not known. To gain confidence in miR-124 targets, we combined the precisions f(t) from three databases (DIANA, PicTAR and TargetScan) and cross-referenced them against our known differential proteomic list, which led us identify guanine nucleotide binding protein alpha inhibitor 1 (GNAI1) as a miR-124 target. GNAI1, or sometimes referred to as Gαi1, is an adenylate cyclase inhibitor, which subsequently decreases the metabolism of ATP to cAMP. The cAMP is a second messenger and mediator of the cAMP/PKA/CREB pathway. Fig. 2b shows the given scores from each prediction algorithm specifically for miR-124 targeting GNAi1: DIANA has a score of 0.67 or 67% chance that the prediction is correct; TargetScan reports an aggregate Pct score or the combined probability of all predicted target sites for a given miRNA to a target of 0.6154; PicTar provides a single score value of 37, which we normalized over the highest score in the prediction data set, to 0.19. We assume that the precision scores are independent and combined precision, or f(t) for miR-124 to target GNAI1 is 0.9 or 90% confidence. A point to note is that even with a high f(t), it may not translate directly to actual biological situations as such prediction engines are never
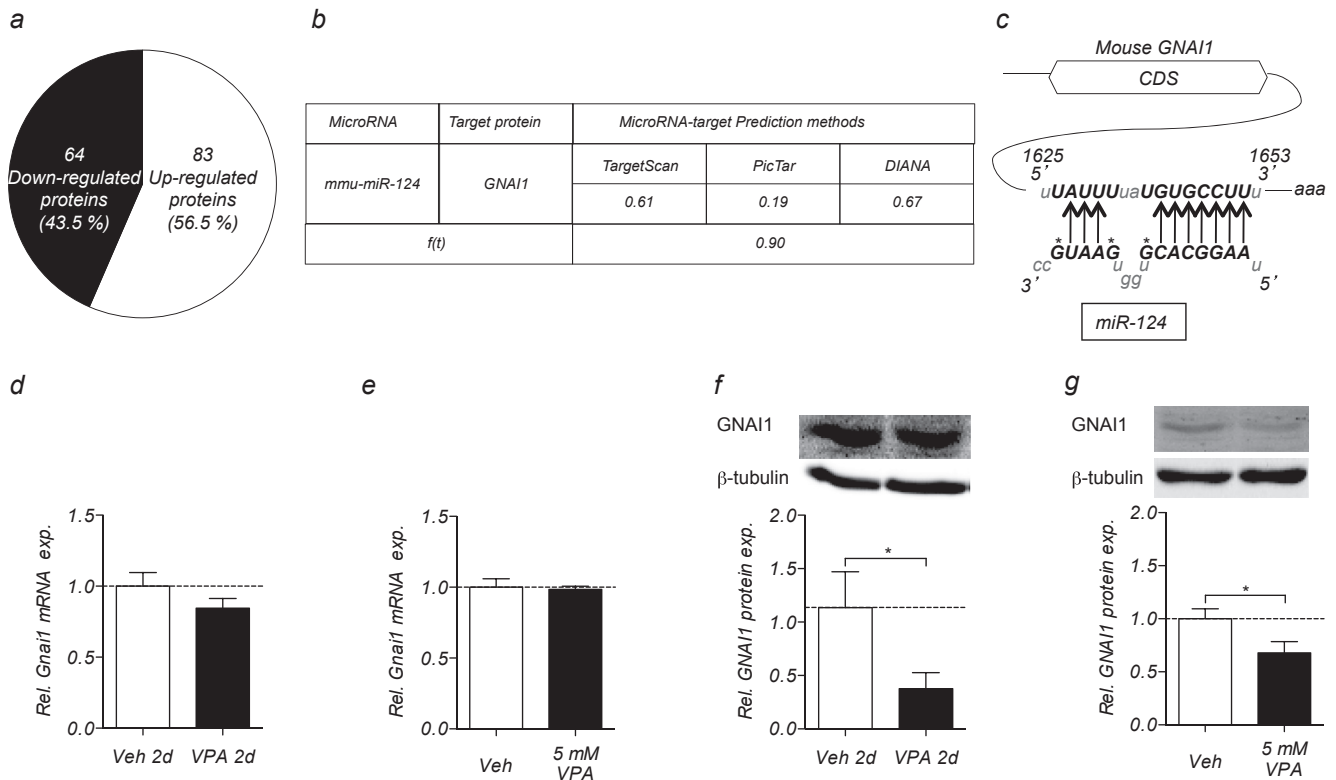
Fig. 2. VPA downregulates GNAI1 protein *in vivo* and *in vitro*. (a) Pie chart showing the differential expression of proteins *in vivo* after Veh 2d or VPA 2d obtained from iTRAQ analysis (up-regulated, white sector; down-regulated, black sector). (b) Candidate down-regulated protein, Guanine Nucleotide binding protein, Alpha Inhibiting 1 (GNAI1), was predicted *in silico* with TargetScan, PicTar and DIANA databases to be the potential target protein of miR-124. (c) Schematic miR-124 binding site of GNAI1 sequence. (d) Validation of *Gnai1* by real-time qPCR *in vivo* after Veh 2d or VPA 2d. *Gnai1* mRNA slightly decreases. (e) Validation of *Gnai1* by real-time qPCR *in vitro* after Veh or VPA treatment. *Gnai1* mRNA does not change. (f) Reduction in GNAI1 protein *in vivo* after Veh 2d or VPA 2d. (g) Significant reduction of GNAI1 protein *in vitro* VPA treatment (Veh, white bars, n = 3; VPA, black bars, n = 3). Data are represented as means ± s.e.m., normalized to *18S* and *Gapdh* or βIII-tubulin and relative to Veh, *p < 0.05.

benchmarked against real data, thus it is important to validate this data, which we did in the following figures, using the *in vitro* system. We schematically depict the binding site location for miR-124 to the 3′ end of GNAI1 (Fig. 2c) that could repress its post-translation.

3.5. Translation of Gnai1 is affected after VPA administration

To understand if the down-regulation of GNAI1 protein is at the transcription or the translation level, we next checked the expression of *Gnai1* mRNA both *in vivo* and *in vitro* after VPA administration. There was no significant decrease in mRNA levels in both *in vivo* and *in vitro* conditions (Fig. 2d and e, n = 3; p = 0.1089, p = 0.8278, respectively). We also checked the GNAI1 protein level in both the mouse visual cortices and in primary neuronal cultures. Indeed, GNAI1 was significantly decreased in both *in vivo* (Fig. 2f, n = 4, p = 0.0253) and *in vitro* (Fig. 2g, n = 3, p = 0.0402) conditions. This suggests that translational repression, and not transcriptional repression of *Gnai1* was affected after VPA administration.

3.6. Selective inhibition of miRNA-124 regulate GNAI1 protein in vitro

To investigate the direct relationship of miR-124 with GNAI1, we pretreated the primary neuronal culture with a selective miR-124 inhibitor. We confirmed the efficacy of the miR-124 inhibitor and 3 DIV neuronal cultures pretreated with miR-124 inhibitor have lower miR-124 expression level (Fig. 3a, n = 3, p = 0.0059). Next, we prepared whole cell protein lysates and checked the GNAI1

protein expression level by western blotting analysis. With the inhibition of miR-124, GNAI1 protein was increased (Fig. 3b, n = 7, p = 0.0504).

3.7. Selective miRNA-124 mimic regulate GNAI1 protein in vitro

To further verify the direct relationship of miR-124 with GNAI1, we also pretreated primary neuronal culture with a selective miR-124 mimic and observed a significant increase in miR-124 expression level (Fig. 3c, n = 3—4, p = 0.0257). We checked the GNAI1 protein expression level in whole cell lysates by western blot and GNAI1 was significantly decreased after miR-124 mimic treatment (Fig. 3d, n = 4, p = 0.0320).

3.8. VPA increases cAMP and Bdnf expression

As GNAI1 is an adenylate cyclase inhibitor, its reduction should increase the levels of adenylyl cyclase activity. We next checked on the levels of cyclic adenosine 3′, 5′ —monophosphate (cAMP) after VPA stimulation and it was indeed increased after VPA stimulation (Veh: white bar; 5 mM VPA treatment: black bar, Fig. 4a, n = 3, p = 0.0743). We tested out the relationship of cAMP to miR-124 and GNAI1 and we found that the inhibition of miR-124 decreased cAMP levels and cAMP levels subsequently increased by 4-fold when GNAI1 was inhibited (Veh: white bar; 5 mM VPA treatment: black bar, Fig. 4b and c, n = 3, p = 0.0563, p = 0.026).

cAMP is a critical modulator of synaptic plasticity and its activation stimulates adenylyl cyclases to induce downstream gene transcription, such as brain-derived neurotrophic factor or BDNF
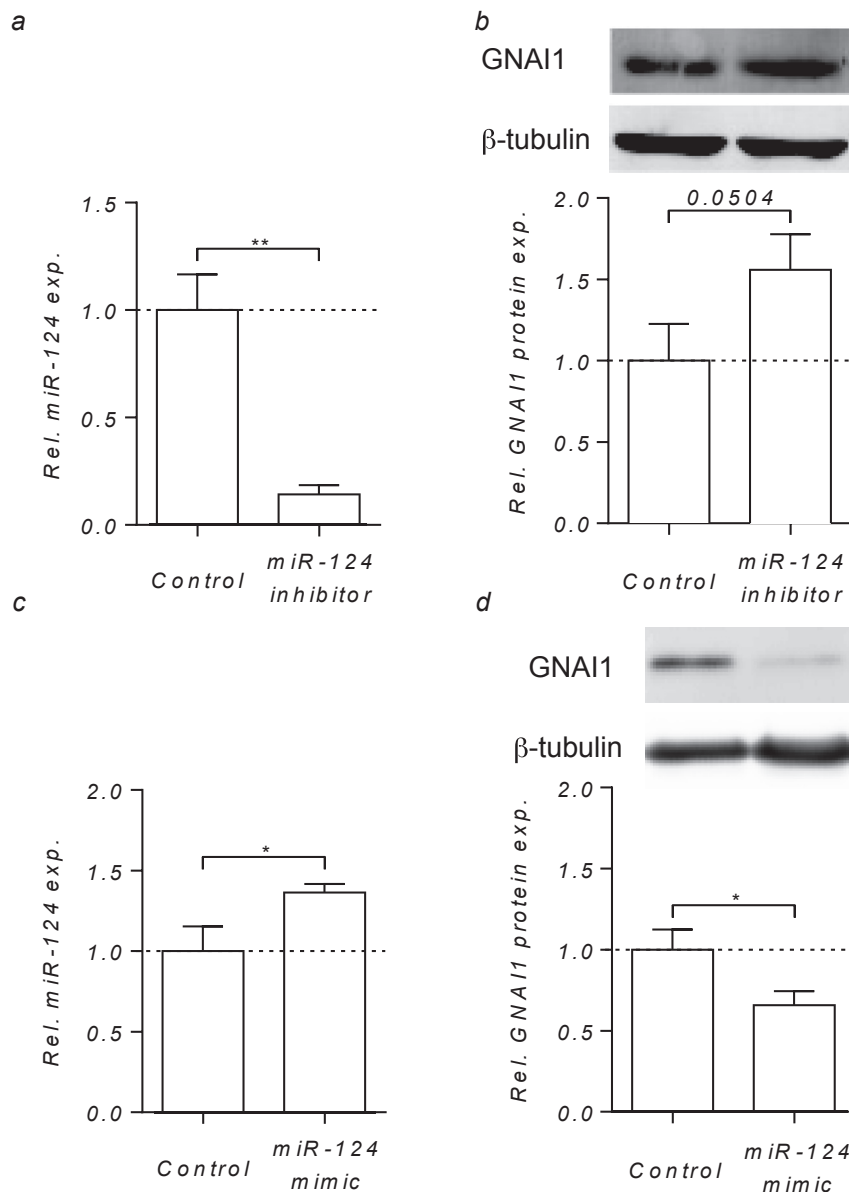
Fig. 3. VPA mediates its action through miR-124 to downregulate GNAI1. (a) Reduction of miR-124 after the addition of miR-124 inhibitor *in vitro* (n = 3, **p < 0.01). (b) Primary neuronal cultures treated with miRNA-124 inhibitor shows an increase in GNAI1 protein (n = 7, p = 0.0504). (c) The addition of miR-124 mimic increases miR-124 levels (n = 3–4, *p < 0.05). (d) miR-124 mimic significantly decrease GNAI1 protein (n = 4, *p < 0.05). Data are represented as means ± s.e.m., normalized to *5S* and *U6* or βIII-tubulin and relative to Control.

(Mizuno et al., 2002; Shelly et al., 2010). BDNF is a well-known nerve growth factor that increases neurogenesis and synaptic plasticity (Einat et al., 2003; Laeng et al., 2004; Rosenberg, 2007). We then checked *Bdnf* mRNA expression after Veh or VPA administration and found their levels to be enhanced (Veh: white bar; 5 mM VPA treatment: black bar, Fig. 4d, n = 3–4, p = 0.0436). We investigated if reduction of miR-124 or GNAI1 would affect the expression levels of *Bdnf*. Indeed, we found *Bdnf* mRNA was decreased with miR-124 inhibition but increased with *Gnai1* siRNA by 2.5-fold (Veh: white bar; 5 mM VPA treatment: black bar, Fig. 4e and f, n = 3, p = , p = 0.0007).

3.9. Inhibition of miR-124 prevents GNAI1 down-regulation after VPA in vitro

To test if miR-124 is important in regulating the levels of GNAI1

or BDNF, we pretreated primary neuronal cultures with miR-124 inhibitor and applied either Veh or 5 mM VPA to them. After a 12-h stimulation, the cells were harvested and whole cell protein samples were extracted for western blot analysis. Thus, pretreatment of miR-124 inhibitor block miR-124 expression that prevent GNAI1 and *Bdnf* expression, even in the presence of VPA (Veh: white bar; 5 mM VPA treatment: black bar, Fig. 5a and c, n = 3, p = 0.733, p = 0.917 respectively). This experiment strengthens the link between that miR-124-GNAI1-*Bdnf* cascade.

We then added VPA to primary neuronal culture pretreated with miR-124 mimic and checked the GNAI1 protein expression level. The addition of miR124 mimic further enhanced the reduction of GNAI1 protein level after VPA stimulation, suggesting that miR-124 directly repress GNAI1 protein translation and conversely upregulates *Bdnf* mRNA (Veh: white bar; 5 mM VPA treatment: black bar, Fig. 5b and d, n = 3, p = 0.0053 and p = 0.0277). This strengthens
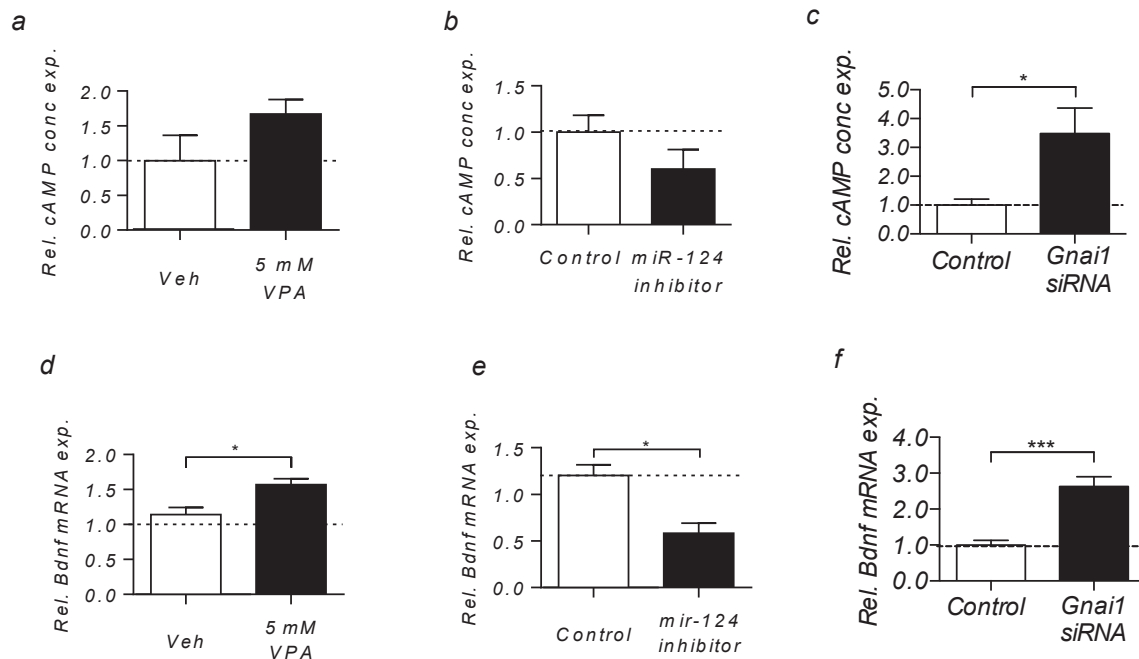
Fig. 4. VPA up-regulates Bdnf mRNA through cAMP *in vitro*. (a) VPA increases cAMP concentration, (b) miR-124 inhibition also increases cAMP concentration, and (c) *Gnai1* inhibition increases cAMP concentration, in primary neuronal culture (vehicle, white bar; VPA, black bar; n = 3–5, *p < 0.05) (d) VPA stimulates significant up-regulation of *Bdnf* mRNA after VPA treatment *in vitro*, (e) miR-124 inhibitor stimulates significant down-regulation of *Bdnf* mRNA *in vitro* and (f) *Gnai1* siRNA stimulates significant up-regulation of *Bdnf* mRNA *in vitro* (Veh, white bars, n = 4; VPA, black bars, n = 3, *p < 0.05). Data are represented as means ± s.e.m., normalized to *Gapdh* and relative to Veh, unpaired student *t*-test, *p < 0.05.

our hypothesis that VPA acts through miR-124 to down-regulate GNAI1.

4. Discussion & conclusions

This study generated five main findings: 1) VPA induces miR-124 and down-regulates GNAI1; 2) miR-124 mimic down-regulates GNAI1 whilw inhibiting miR-124 increases GNAI1; 3) VPA activates cAMP and induces *Bdnf* and this pathway can also be induced with *Gnai* siRNA knockdown; 4) VPA, miR-124 mimic and *Gnai1* siRNA knockdown gives rise to *Bdnf* mRNA transcription and the converse with miR-124 inhibition; whereas 5) inhibiting miR-124 abolishes the downstream pathway. Based on our findings, we schematically depict the molecular mechanisms underlying VPA and its effects on BDNF (Fig. 6). After receiving VPA stimulation, miR-124 is induced in nucleus (Fig. 6-1). The induced miR-124 subsequently down regulates GNAI1 expression (Fig. 6-2) and increases adenylyl cyclases activity to elevate cAMP concentration (Fig. 6-3 and 6-4). The elevated cAMP activates signaling pathways causing a downstream gene transcription that increases *Bdnf* expression (Fig. 6-5). There could be signaling pathways that activate *Bdnf* could be further investigated.

Despite using VPA in clinical settings for the last few decades, its exact mechanism is still unknown. While it is mainly used as an anticonvulsant, VPA has been shown to have other therapeutic effects such as anti-tumorogenesis, neuroprotective, promoting neurogenesis, differentiation and neuroregeneration and improving synaptic plasticity (Abematsu et al., 2010; Foti et al., 2013; Fukuchi et al., 2009; Hao et al., 2004; Jessberger et al., 2007; Laeng et al., 2004; Liu et al., 2012; Morris and Monteggia, 2013; Phiel et al., 2001). We are interested in the underlying molecular mechanism of VPA that increases neuroplasticity. Studies have shown that VPA induces neurotrophins, in particular, brain-derived neurotrophic factor (BDNF) (Nishino et al., 2012). BDNF is

well established to direct growth and differentiation in the developing nervous system, promotes neurogenesis and dendritic spine reorganization and activity-dependent plasticity in adult brain [16–18(Nishino et al., 2012). Thus, we elucidated the molecular mechanism of VPA and its mediation of *Bdnf* transcription.

VPA has been reported to induce epigenetic changes such as inhibiting histone deacetylases and inducing microRNAs that modulate gene expression changes (Goh et al., 2011; Hunsberger et al., 2012; Jessberger et al., 2007; Tremolizzo et al., 2005; Zhou et al., 2008). The interplay between HDACs and miRNAs is tightly regulated and is evident from our recent report, whereby we predicted *in silico* the miRNAs network that interact and disrupt protein complexes after VPA administration (Goh et al., 2011). While VPA is a pan-HDAC inhibitor that inhibits both class I and IIa HDAC enzymes (Jessberger et al., 2007; Tremolizzo et al., 2005; Yasuda et al., 2009), we and other groups have shown that VPA induces miRNAs in the brain (Hunsberger et al., 2012; Zhou et al., 2008). It is likely that miRNAs could affect epigenetic machinery and in turn, miRNA expression could also be controlled by other epigenetic mechanisms not explored in this study.

The first important finding from our study is identifying VPA-mediated up-regulation of miR-124 targeting at GNAI1 (Figs. 1 and 2). First, the change in miRNAs after VPA administration were screened and the data segregates very well into the respective treatment groups (Suppl. Fig. 1). We validated the VPA-induced miRNAs in both *in vivo* and *in vitro* systems (Fig. 1). miRNAs comprise short noncoding RNA that regulate gene expression post-transcriptionally and many of their target proteins are usually predictive but lacking a solid benchmark of their exact precisions. Thus, to gain confidence of our findings, we used a combination of algorithms and we cross-referenced them against our known differential proteomic list. This led to finding miR-124 targeting guanine nucleotide binding protein alpha inhibitor 1 protein (GNAI1, Fig. 2b), an adenylyl cyclase inhibitor (Bromberg et al., 2011; Pineda
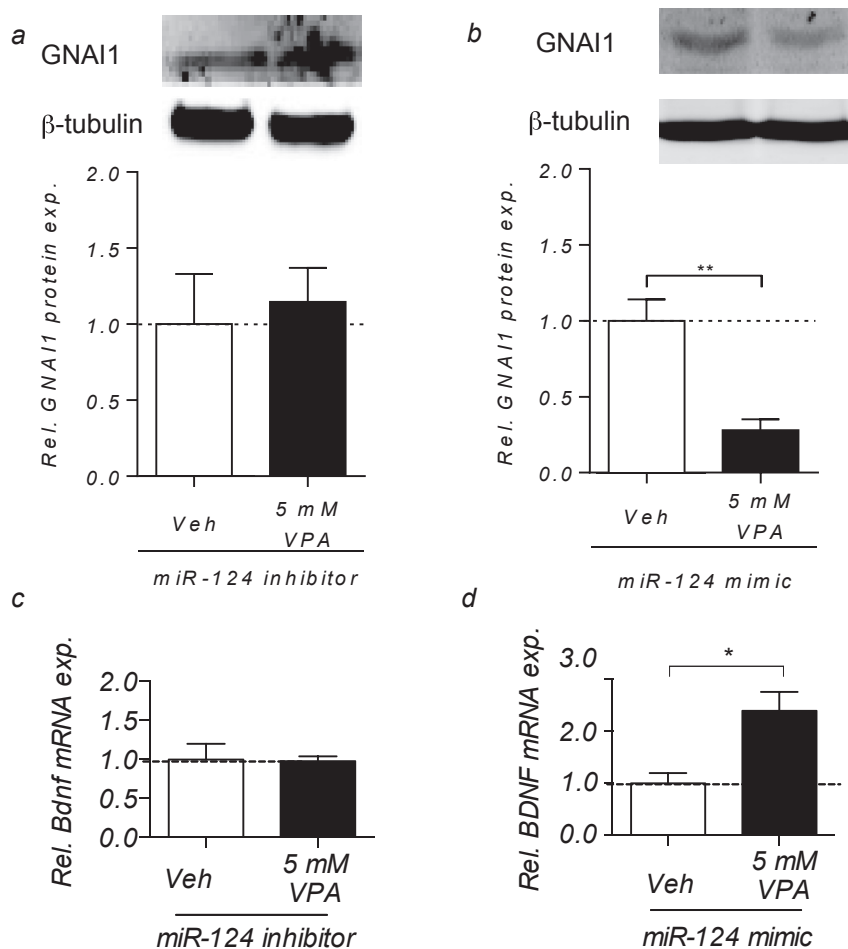
Fig. 5. miR-124 inhibition blocks the downregulation of GNAI1 and BDNF by VPA. (a) miR-124 inhibition blocks the degradation of GNAI1 level *in vitro* (culture pretreated with miR-124 inhibitor; vehicle, white bar; VPA, black bar; n = 3). (b) The addition of miR-124 mimic enhances the efficacy of VPA to degrade GNAI1 level *in vitro* (culture pretreated with miR-124 mimic; Veh, white bar; VPA, black bar; n = 3). (c) VPA stimulation in miR-124 inhibited cultures did not show any difference in *Bdnf* mRNA expression level (Pretreatment with inhibitor, Veh, white bar; VPA, black bar; n = 3). (d) VPA stimulation in cultures treated with miR-124 mimic showed an augmented increase in *Bdnf* mRNA expression level (Veh, white bar; VPA, black bar; n = 3, $^{*}p \leq 0.05$). Data are represented as means ± s.e.m., normalized to *Gapdh* or βIII-tubulin and relative to Veh, unpaired student t-test, $^{*}p < 0.05$, $^{**}p \leq 0.01$.

et al., 2004; Sunahara et al., 1996; Wettschureck and Offermanns, 2005). By using either miR-124 mimic or inhibitor, the levels of GNAI1 either down- or up-regulate, respectively, further supporting their relationship (Fig. 3).

Heterotrimeric G-proteins transduce molecular signals from hormones, neurotransmitters, and chemokines and convert them into intracellular responses through G-protein coupled receptors to modulate physiological functions, such as learning and memory (Bromberg et al., 2011; Wettschureck and Offermanns, 2005). G-proteins consist of alpha, beta, and gamma subunits and the alpha subunit plays an important role in binding guanine nucleotides to hydrolyze GTP to GDP. There are about twenty different α–subunits identified in the mammalian heterotrimeric G-protein superfamily and ubiquitously expressed in the brain (Bromberg et al., 2011; Wettschureck and Offermanns, 2005). GNAI1 is an adenylyl cyclase inhibitor and its inhibition will cause the accumulation of cAMP within the cell. The ablation of GNAI1 has been shown to increase hippocampal adenylyl cyclase activity and enhances long-term potentiation (LTP) in area CA1 (Pineda et al., 2004). cAMP is a critical modulator of synaptic plasticity and is known to induce gene transcription by mediating through activation of cAMP to activate downstream gene transcription. BDNF is a well-known neurotrophin that is important in neurogenesis (Mizuno et al.,

2002; Rosenberg, 2007). In fact, chronic concomitant administration of VPA and lithium modulates neuroplasticity molecules through the BDNF transcription (Nishino et al., 2012). We obtained similar result in our 2-day VPA treatment *in vivo* (manuscript in submission). We propose that VPA induces miR-124 that inhibits GNAI1. This leads to increase cAMP level and increase in *Bdnf* transcription.

The association between miR-124 and BDNF has previously been established (Nishino et al., 2012). While we and other groups have shown that VPA treatment induced miR-124 and consequently increased *Bdnf* (Fig. 4d–f), we wanted to verify if the up-regulation of *Bdnf* is a result of miR-124. With a miR-124 inhibitor, *Bdnf* transcription decreased (Fig. 4e). Even in the presence of VPA, miR-124-inhibited primary cortical cultures could not increase *Bdnf*, suggesting that miR-124 is needed for the VPA induced up-regulation of *Bdnf* (Fig. 5c). In addition, we demonstrated the next important finding where GNAI1 acts as an intermediary from miR-124 to BDNF. By knocking down GNAI1 with siRNA, levels of BDNF can be increased (Fig. 4f), suggesting the role of GNAI1 in BDNF regulation, though we cannot rule out that there are other signaling pathways that may activate cAMP independent of GNAI1. Taken together, our findings support the role of both miR-124 and GNAI1 in BDNF regulation. Since changes in the levels and activities of
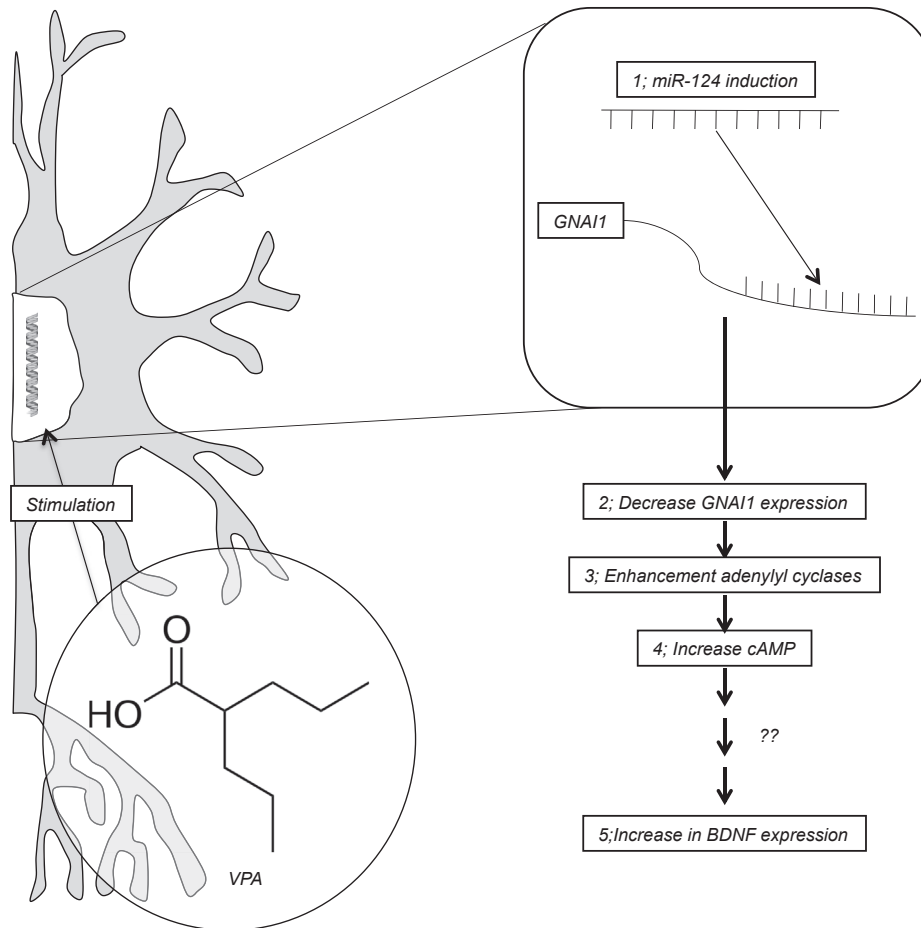
Fig. 6. Schematic representation of the molecular mechanistic action of VPA mediated through miR-124 and reduction of GNAI1 protein. Upon VPA stimulation, miR-124 is induced and binds to 3′UTR sequence of Gnai1 protein. This, in turn, down-regulates GNAI1 protein synthesis. The reduced GNAI1 increases cAMP, which in turn, increases BDNF after VPA stimulation. There are additional signaling pathways, which may activate BDNF.

BDNF have been described in a number of neurodegenerative disorders, we also checked GNAI1 protein expression level in a mouse model of Huntington's disease. Preliminary results show that GNAI1 protein was significantly increased in the cerebral cortices (unpublished data, data not shown). This suggests the possible usage of either miR-124 inhibitor or Gnai1 siRNA in the treatment of neurodegenerative diseases through elevation of BDNF levels.

In summary, we have identified a molecular mechanism through VPA that induces BDNF under miR-124 control and its target protein, GNAI1. In the last few years, the National Clinical and Translational Science (http://www.ncats.nih.gov/) has been collaboratively testing new therapeutic uses for existing pharmaceutical agents in a drug-repurposing program. With the available information on the pharmacology, formulation and potential toxicity of VPA, this may prove to be easier for its integration into health care therapy for neurological diseases and beyond its current use in epilepsy and depression.

The implication of miR-124→GNAI1→BDNF pathway with valproic acid treatment suggests that we could repurpose an old drug, valproic acid, as a clinical application to elevate neurotrophin levels in treating neurodegenerative diseases. This study represents only the first steps toward the unique mechanisms used by miRNAs and their target transcripts. Nonetheless, it contributes to our understanding of miRNAs and their functions in regulatory to generation sequencing, its accessibility and cost-effectiveness, selective screening of miRNAs directly on the human transcriptomic" may become a routine procedure for diagnosis and personalized medicine in the near future.

Conflict of interest statement

The authors declare no conflict of interest.

Authorship contributions

HO and VL performed the experiments and analyzed the data; WG and LW analyzed the proteomics data; HO and JS designed the research study. HO and JS wrote the paper.

Appendix A. Supplementary data

Supplementary data related to this article can be found at http://dx.doi.org/10.1016/j.neuint.2015.10.010.

References

Abematsu, M., Tsujimura, K., Yamano, M., Saito, M., Kohno, K., Kohyama, J., et al., 2010. Neurons derived from transplanted neural stem cells restore disrupted neuronal circuitry in a mouse model of spinal cord injury. J. Clin. Investig. 120, 3255–3266.

Bredy, T.W., Wu, H., Crego, C., Zellhoefer, J., Sun, Y.E., Barad, M., 2007. Histone modifications around individual BDNF gene promoters in prefrontal cortex are associated with extinction of conditioned fear. Learn. Mem. 14, 268–276.

Bromberg, K.D., Iyengar, R., He, J.C., 2011. Regulation of neurite outgrowth by G signaling pathways. Front. Biosci. 13, 4544–4557.

Calabrese, F., Luoni, A., Guidotti, G., Racagni, G., Fumagalli, F., Riva, M.A., 2012. Modulation of neuronal plasticity following chronic concomitant administration of the novel antipsychotic lurasidone with the mood stabilizer valproic acid. Psychopharmacology 226, 101–112.

Cao, X., Pfaff, S.L., Gage, F.H., 2007. A functional study of miR-124 in the developing neural tube. Genes Dev. 21, 531–536.

Cheng, L.-C., Pastrana, E., Tavazoie, M., Doetsch, F., 2009. miR-124 regulates adult neurogenesis in the subventricular zone stem cell niche. Nat. Neurosci. 12, 399–408.

Chuang, J.C., Jones, P.A., 2007. Epigenetics and microRNAs. Pediatr. Res. 61, 24R–29R.

Das, E., Jana, N.R., Bhattacharyya, N.P., 2013. MicroRNA-124 targets CCNA2 and regulates cell cycle in STHdhQ111/HdhQ111 cells. Biochem. Biophys. Res. Commun. 437, 217–224.

Edbauer, D., Neilson, J.R., Foster, K.A., Wang, C.-F., Seeburg, D.P., Batterton, M.N., et al., 2010. Regulation of synaptic structure and function by FMRP-associated microRNAs miR-125b and miR-132. Neuron 65, 373–384.

Einat, H., Yuan, P., Gould, T.D., Li, J., Du, J., Zhang, L., et al., 2003. The role of the extracellular signal-regulated kinase signaling pathway in mood modulation. J. Neurosci. Off. J. Soc. Neurosci. 23, 7311–7316.

Filipowicz, W., Bhattacharyya, S.N., Sonenberg, N., 2008. Mechanisms of post-transcriptional regulation by microRNAs: are the answers in sight? Nat. Rev. Genet. 2008, 102–114.

Fiore, R., Khudayberdiev, S., Saba, R., Schratt, G., 2011. MicroRNA function in the nervous system. Prog. Mol. Biol. Transl. Sci. 102, 47–100.

Foti, S.B., Chou, A., Moll, A.D., Roskams, A.J., 2013. HDAC inhibitors dysregulate neural stem cell activity in the postnatal mouse brain. Int. J. Dev. Neurosci. 31, 434–447.

Friedman, R.C., Farh, K.K.H., Burge, C.B., Bartel, D.P., 2008. Most mammalian mRNAs are conserved targets of microRNAs. Genome Res. 19, 92–105.

Fukuchi, M., Nii, T., Ishimaru, N., Minamino, A., Hara, D., Takasaki, I., et al., 2009. Valproic acid induces up- or down-regulation of gene expression responsible for the neuronal excitation and inhibition in rat cortical neurons through its epigenetic actions. Neurosci. Res. 65, 35–43.

Gangaraju, V.K., Lin, H., 2009. MicroRNAs: key regulators of stem cells. Nat. Rev. Mol. Cell Biol. 10, 116–125.

Goh, W.W., Sergot, M.J., Sng, J.C., Wong, L., 2013. Comparative network-based recovery analysis and proteomic profiling of neurological changes in valproic acid-treated mice. J. Proteome Res. 12, 2116–2127.

Goh, W.W.B., Oikawa, H., Sng, J.C.G., Sergot, M., Wong, L., 2011. The role of miRNAs in complex formation and control. Bioinformatics 28, 453–456.

Gong, Y., Wu, C.N., Xu, J., Feng, G., Xing, Q.H., Fu, W., et al., 2013. Polymorphisms in microRNA target sites influence susceptibility to schizophrenia by altering the binding of miRNAs to their targets. Eur. Neuropsychopharmacol. 23, 1182–1189.

Hao, Y., Creson, T., Zhang, L., Li, P., Du, F., Yuan, P., et al., 2004. Mood stabilizer valproate promotes ERK pathway-dependent cortical neuronal growth and neurogenesis. J. Neurosci. 24, 6590–6599.

Henry, T.R., 2003. The history of valproate in clinical neuroscience. Psychopharmacol. Bull. 37 (Suppl. 2), 5–16.

Hunsberger, J.G., Fessler, E.B., Wang, Z., Elkahloun, A.G., Chuang, D.-M., 2012. Post-insult valproic acid-regulated microRNAs potential targets for cerebral ischemia. Am. J. Transl. Res. 4, 316–332.

Impey, S., Davare, M., Lasiek, A., Fortin, D., Ando, H., Varlamova, O., et al., 2010. An activity-induced microRNA controls dendritic spine formation by regulating Rac1-PAK signaling. Mol. Cell. Neurosci. 43, 146–156.

Jessberger, S., Nakashima, K., Clemenson, G.D., Mejia, E., Mathews, E., Ure, K., et al., 2007. Epigenetic modulation of seizure-induced neurogenesis and cognitive decline. J. Neurosci. 27, 5967–5975.

Karr, J., Vagin, V., Chen, K., Ganesan, S., Olenkina, O., Gvozdev, V., et al., 2009. Regulation of glutamate receptor subunit availability by microRNAs. J. Cell Biol. 185, 685–697.

Krek, A., Grün, D., Poy, M.N., Wolf, R., Rosenberg, L., Epstein, E.J., et al., 2005. Combinatorial microRNA target predictions. Nat. Genet. 37, 495–500.

Laeng, P., Pitts, R.L., Lemire, A.L., Drabik, C.E., Weiner, A., Tang, H., et al., 2004. The mood stabilizer valproic acid stimulates GABA neurogenesis from rat forebrain stem cells. J. Neurochem. 91, 238–251.

Lagos-Quintana, M., Rauhut, R., Yalcin, A., Meyer, J., Lendeckel, W., Tuschl, T., 2002. Identification of tissue-specific microRNAs from mouse. Curr. Biol. 12, 735–739.

Lim, L.P., Lau, N.C., Garrett-Engele, P., Grimson, A., Schelter, J.M., Castle, J., et al., 2005. Microarray analysis shows that some microRNAs downregulate large numbers of target mRNAs. Nature 433, 769–773.

Liu, X.S., Chopp, M., Kassis, H., Jia, L.F., Hozeska-Solgot, A., Zhang, R.L., et al., 2012. Valproic acid increases white matter repair and neurogenesis after stroke. Neuroscience 220, 313–321.

Makeyev, E.V., Zhang, J., Carrasco, M.A., Maniatis, T., 2007. The microRNA miR-124 promotes neuronal differentiation by triggering brain-specific alternative pre-mRNA splicing. Mol. Cell 27, 435–448.

Maragkakis, M., Reczko, M., Simossis, V.A., Alexiou, P., Papadopoulos, G.L., Dalamagas, T., et al., 2009. DIANA-microT web server: elucidating microRNA functions through target prediction. Nucleic Acids Res. 37, W273–W276.

Mizuno, M., Yamada, K., Maekawa, N., Saito, K., Seishima, M., Nabeshima, T., 2002. CREB phosphorylation as a molecular marker of memory processing in the hippocampus for spatial learning. Behav. Brain Res. 133, 135–141.

Morris, M.J., Monteggia, L.M., 2013. Unique functional roles for class I and class II histone deacetylases in central nervous system development and function. Int. J. Dev. Neurosci. 31, 370–381.

Nelson, P.T., Wang, W.-X., Rajeev, B.W., 2008. MicroRNAs (miRNAs) in neurodegenerative diseases. Brain Pathol. 18, 130–138.

Nishino, S., Ohtomo, K., Numata, Y., Sato, T., Nakahata, N., Kurita, M., 2012. Divergent effects of lithium and sodium valproate on brain-derived neurotrophic factor (BDNF) production in human astrocytoma cells at therapeutic concentrations. Prog. Neuro Psychopharmacol. Biol. Psychiatry 39, 17–22.

Novina, C.D., Sharp, P.A., 2004. The RNAi revolution. Nature 430 (6996), 161–164.

Papagiannakopoulos, T., Kosik, K.S., 2009. MicroRNA-124: micromanager of neurogenesis. Cell Stem Cell 4, 375–376.

Phiel, C.J., Zhang, F., Huang, E.Y., Guenther, M.G., Lazar, M.A., Klein, P.S., 2001. Histone deacetylase is a direct target of valproic acid, a potent anticonvulsant, mood stabilizer, and teratogen. J. Biol. Chem. 276, 36734–36741.

Pineda, V.V., Athos, J.I., Wang, H., Celver, J., Ippolito, D., Boulay, G., et al., 2004. Removal of Giα1 constraints on adenylyl cyclase in the hippocampus enhances LTP and impairs memory formation. Neuron 41, 153–163.

di Porzio, U., Daguet, M.C., Glowinski, J., Prochiantz, A., 1980 Nov 27. Effect of striatal cells on in vitro maturation of mesencephalic dopaminergic neurones grown in serum-free conditions. Nature 288 (5789), 370–373.

Putignano, E., Lonetti, G., Cancedda, L., Ratto, G., Costa, M., Maffei, L., et al., 2007. Developmental downregulation of histone posttranslational modifications regulates visual cortical plasticity. Neuron 53, 747–759.

Rosenberg, G., 2007. The mechanisms of action of valproate in neuropsychiatric disorders: can we see the forest for the trees? Cell. Mol. Life Sci. 64, 2090–2103.

Ross, P.L., Huang, Y.N., Marchese, J.N., Williamson, B., Parker, K., Hattan, S., et al., 2004. Multiplexed protein quantitation in Saccharomyces cerevisiae using amine-reactive isobaric tagging reagents. Mol. Cell Proteom. 3, 1154–1169.

Sanuki, R., Onishi, A., Koike, C., Muramatsu, R., Watanabe, S., Muranishi, Y., et al., 2011. miR-124a is required for hippocampal axogenesis and retinal cone survival through Lhx2 suppression. Nat. Neurosci. 14, 1125–1134.

Shelly, M., Lim, B.K., Cancedda, L., Heilshorn, S.C., Gao, H., Mm, Poo, 2010. Local and long-range reciprocal Regulation of cAMP and cGMP in axon/dendrite formation. Science 327, 547–552.

Silingardi, D., Scali, M., Belluomini, G., Pizzorusso, T., 2010. Epigenetic treatments of adult rats promote recovery from visual acuity deficits induced by long-term monocular deprivation. Eur. J. Neurosci. 31, 2185–2192.

Sunahara, R.K., Dessauer, C.W., Gilman, A.G., 1996. Complexity and diversity of mammalian adenylyl cyclases. Annu. Rev. Pharmacol. Toxicol. 36, 461–480.

Tremolizzo, L., Doueiri, M.-S., Dong, E., Grayson, D.R., Davis, J., Pinna, G., et al., 2005. Valproate corrects the schizophrenia-like epigenetic behavioral modifications induced by methionine in mice. Biol. Psychiatry 57, 500–509.

Visvanathan, J., Lee, S., Lee, B., Lee, J.W., Lee, S.K., 2007. The microRNA miR-124 antagonizes the anti-neural REST/SCP1 pathway during embryonic CNS development. Genes Dev. 21, 744–749.

Vo, N., Klein, M.E., Varlamova, O., Keller, D.M., Yamamoto, T., Goodman, R.H., et al., 2005. From the cover: a cAMP-response element binding protein-induced microRNA regulates neuronal morphogenesis. Proc. Natl. Acad. Sci. U. S. A. 102, 16426–16431.

Wayman, G.A., Davare, M., Ando, H., Fortin, D., Varlamova, O., Cheng, H.Y.M., et al., 2008. An activity-regulated microRNA controls dendritic plasticity by down-regulating p250GAP. Proc. Natl. Acad. Sci. U. S. A. 105, 9093–9098.

Wettschureck, N., Offermanns, S., 2005. Mammalian G proteins and their cell type specific functions. Physiol. Rev. 85, 1159–1204.

Yasuda, S., Liang, M.H., Marinova, Z., Yahyavi, A., Chuang, D.M., 2009. The mood stabilizers lithium and valproate selectively activate the promoter IV of brain-derived neurotrophic factor in neurons. Mol. Psychiatry 14, 51–59.

Yu, J.-Y., Chung, K.-H., Deo, M., Thompson, R.C., Turner, D.L., 2008. MicroRNA miR-124 regulates neurite outgrowth during neuronal differentiation. Exp. Cell Res. 314, 2618–2633.

Zhou, R., Yuan, P., Wang, Y., Hunsberger, J.G., Elkahloun, A., Wei, Y., et al., 2008. Evidence for selective microRNAs and their effectors as common long-term targets for the actions of mood stabilizers. Neuropsychopharmacology 34, 1395–1405.